Wheat straw based polygeneration systems integrating the electricity, heating and transport sector

Kofler, René; Clausen, Lasse Røngaard

Published in:
Smart Energy

Link to article, DOI:
10.1016/j.segy.2021.100015

Publication date:
2021

Document Version
Publisher's PDF, also known as Version of record

Smart Energy 2 (2021) 100015

Contents lists available at ScienceDirect

Smart Energy

journal homepage: www.journals.elsevier.com/smart-energy

Wheat straw based polygeneration systems integrating the electricity, heating and transport sector

René Kofler*, Lasse Røngaard Clausen

Section of Thermal Energy, DTU Mechanical Engineering, Technical University of Denmark, Kgs. Lyngby, Denmark

ARTICLE INFO

Article history:
Received 18 December 2020
Received in revised form
24 March 2021
Accepted 25 March 2021
Available online 30 March 2021

Keywords:
Biofuels
Biorefinery
Biomass gasification
Dimethyl ether (DME)
Electrofuels
Polygeneration
Power-to-gas
Power-to-liquid
Synthetic natural gas (SNG)
Thermodynamic analysis
Wheat straw

ABSTRACT

To achieve a 100% renewable energy system, plants integrating the electricity, heating and transport sectors in a Smart Energy System are required. In this work, three different polygeneration plants producing biofuels and heat, while interacting with the electricity grid are presented. All plants were based on wheat straw gasification in a low temperature circulating fluidized bed gasifier. High quality bio-oil was produced by catalytically upgrading and condensing the tars in the produced gas. Additionally, bio-ash containing carbon was produced, which acts as fertilizer and carbon sequestration when returned to the fields. The three plants used the tar-free gas to produce electricity, synthetic natural gas (SNG) and dimethyl ether (DME), respectively. The electricity producing plant delivered electricity to the grid, while the SNG and DME production plants used electricity for producing electrolytic hydrogen to boost the fuel production. The plants were evaluated using energy and carbon efficiencies. The analysis showed that all plants achieved total energy efficiencies >83%, including process heat and district heating as by-products. The SNG production plant yielded the highest carbon efficiency (91%) of carbon bound in bio-fuels and bio-ash, followed by the DME (50%) and the electricity production plant (23%).

1. Introduction

In order to reduce CO_2-emissions and thereby the human impact on climate change, a transition from the fossil fuel based to a renewable energy system is necessary. This requires changes in all sectors, including electricity, heating and transport sectors. The integration of the different sectors in a Smart Energy System was presented by Lund et al. [1], who state that a shift away from single-sector thinking towards a holistic approach will help in finding the least-cost strategies towards a 100% renewable energy system. Mathiesen et al. [2] showed that the concept of Smart Energy Systems enables the design of 100% renewable energy and transport solutions. These solutions are based on fluctuating renewable energy sources such as wind, solar, wave power and low value heat sources and the use of biomass for producing transport fuels for heavy transport, shipping and aircrafts. When using biomass for energetic purposes, the sustainable use of available resources needs to be ensured in order to avoid negative effects on the environment through competition with the food industry, deforestation and changes in land-use [3]. A promising way of avoiding or limiting these effects is the use of residual biomass. Residual biomass is commonly used to define by-products with no further value in the food, farming and wood industry. The energy potential of residual biomass from agriculture in Denmark corresponds to 14–19% of the total primary energy consumption in 2015 [4]. Venturini et al. [4] showed that in future carbon- and resource-constrained scenarios in Denmark, the use of residual biomass resources like wheat straw in biorefineries with gasification is very attractive to supply the heavy segments of the transport sector. However, gasification of agricultural biomass residues, such as straw or manure, is challenging, because of the high content of ash compounds and their low melting temperature.

The low temperature circulating fluidized bed (LT-CFB) gasifier was developed by Danish Fluid Bed Technology in collaboration

* Corresponding author.
E-mail address: renekof@mek.dtu.dk (R. Kofler).

https://doi.org/10.1016/j.segy.2021.100015

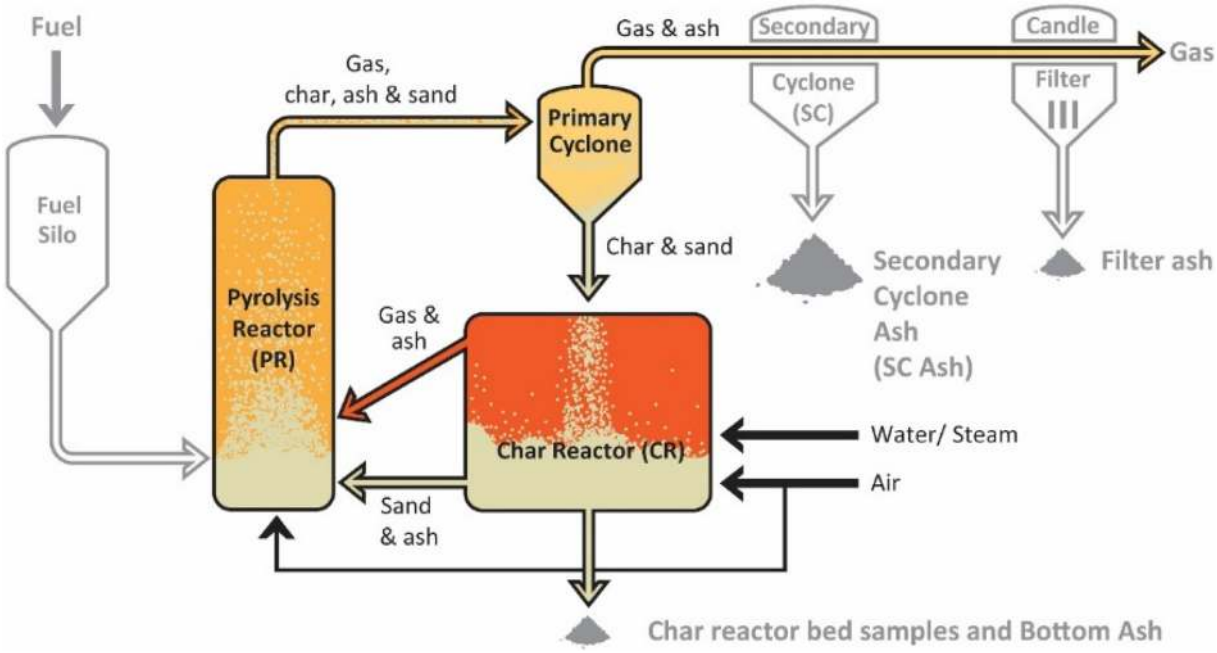

Fig. 1. Sketch of Low-Temperature Circulating Fluidized Bed (LT-CFB) gasifier [8].

with the Technical University of Denmark (DTU) and DONG energy (now called Ørsted) [5]. Fig. 1 depicts a sketch of the LT-CFB gasifier. The gasifier has been designed for efficient gasification of agricultural residues. It consists of two separate reactors for pyrolysis and char gasification, respectively. Sand is used as bed material in the reactors and is circulated between the pyrolysis and the char reactor. Thereby, it acts as heat transfer medium to transfer the required heat from the char reactor to the pyrolysis reactor. By keeping the temperature below the melting point of the ash compounds (700–750 °C), agglomeration problems in the gasifier can be avoided. In addition to its ability to process agricultural residues, the LT-CFB gasifier is able to produce valuable bio-ashes or biochar, which can be used as fertilizer, soil amendment and carbon sequestration [6], thereby contributing to reduce greenhouse gas emissions from agriculture [7]. The LT-CFB gasifier (alias Pyroneer) has been successfully upscaled to 6 MW_{th} by DONG Energy in Kalundborg, Denmark. Here, the gas from the gasifier was used for co-firing an existing coal power plant. The technology can potentially be scaled in sizes of 5–100 MW input depending on the fuel [5].

The relatively low gasification temperatures of the LT-CFB gasifier result in a high tar content in the produced gas. This makes it unsuitable for direct use for synthesis processes or electricity production through gas engines, gas turbines or fuel cells. The tars can be removed by cooling the product gas and thereby condensing the tars to bio-oil, which is an additional product of the process. However, high oxygen and moisture contents as well as high acidity make the untreated bio-oil unsuited for direct application. Oxygen content, moisture content and acidity can be reduced by using catalysts for deoxygenating the pyrolysis vapours [9]. However, catalytic treatment reduces the oil yield and leads to coke formation on the catalyst. Experiments with wheat straw [9] showed that the liquid organics separate into two phases after condensation, the so-called bio-oil and aqueous organics. The bio-oil fraction has a low moisture content (<5% after catalytic treatment), while the aqueous organics fraction contains mainly water (>80%).

Fig. 2 shows a simplified sketch of the so-called PolyGas system, consisting of the LT-CFB gasifier, a hot gas filter, a catalytic reactor for deoxygenating the bio-oil and an oil collector, as investigated by Eschenbacher et al. [10]. The system enables the conversion of residual biomass to tar-free gas, bio-oil with low oxygen content and low acidity, and bio-ash. By-products of the system are heat and aqueous organics. The PolyGas system enables the integration of the transport sector and the heating sector through production of biofuels in form of bio-oil and heat. The further utilization of the tar-free gas has not been investigated yet and will be the scope of this work. This enables an integration of the biorefinery with the electricity grid and makes the system potentially a promising actor in Smart Energy Systems.

The simplest way of integrating the biorefinery with the electricity sector is achieved through combustion of the tar-free gas in a gas engine. Depending on the country and the necessities of the electricity grid, the electricity producing plant could act as base load power plant or as operating reserve in the grid.

Another way of integration with the electricity sector is the production of electrofuels by using electricity for producing hydrogen and use it for converting the gas to transport fuels. Previous studies on the LT-CFB gasifier [8,10] showed a high content of methane and other light hydrocarbons in the gas. The presence of these components makes the gas especially suitable for synthetic natural gas (SNG) production. The produced SNG can be injected to the natural gas grid or used as fuel for shipping, aviation or heavy goods transport. Production of SNG through biomass gasification and electrolysis has shown high energy and carbon efficiencies using steam electrolysis [11,12] or co-electrolysis [13–15]. In these studies, SNG was produced synthesizing CO and CO_2 together with hydrogen to methane, using methanation reactors. The investigated feedstock included wood, different manures, sewage sludge and other, however, none of the studies included straw.

Another promising fuel, especially for the shipping sector is dimethyl ether (DME). DME has excellent ignition properties and it can be used in marine Diesel engines without major changes, replacing heavy fuel oil and Diesel [16]. Different studies on producing DME from wood have been conducted. Large-scale production of DME through entrained flow gasification showed high

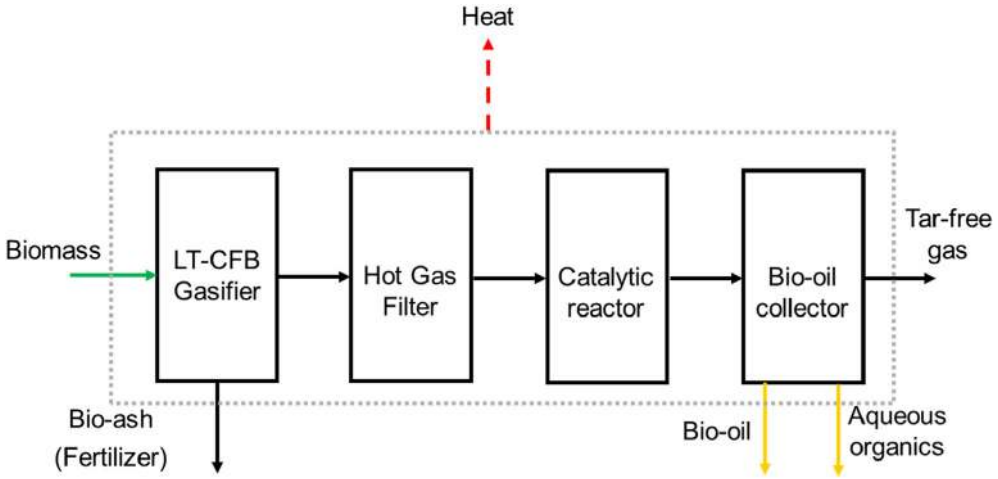

Fig. 2. Simplified sketch of the PolyGas system, converting biomass to tar-free gas, liquid bio-oil and aqueous organics, solid bio-ash, and heat.

energy efficiencies [17]. Small-scale production of DME with two-stage gasification was investigated in Ref. [18]. Addition of co-electrolysis of the syngas in high-temperature solid oxide electrolysis cells was shown in Ref. [19]. Production of DME from wheat straw using the LT-CFB gasifier has not been investigated before.

It was highlighted above that the production of biofuels for the heavy transport sector from residual biomass is crucial for achieving a renewable and sustainable energy systems. In order to achieve optimal integration and be important actors in a Smart Energy System, biofuel production plants need to integrate the electricity, heating and transport sector. This work aims at investigating the possibility of efficiently producing transport fuels from wheat straw through thermal gasification. For this, three novel polygeneration systems based on the PolyGas system, where wheat straw is gasified and the produced tar-free gas is used to produce electricity, SNG and DME, respectively, were assessed. Byproducts of the systems are high quality bio-oil, bio-ashes and heat. Newly developed models for the LT-CFB gasifier and the catalytic upgrading of tars are presented and the systems are assessed through thermodynamic modelling. The performance was evaluated by calculating energy and carbon efficiencies.

2. Design and modelling

In this work, three different ways of using the tar-free gas from the PolyGas system were examined, as seen in Fig. 3. The following plants were investigated:

a) Electricity production plant: The gas from the PolyGas system was combusted in a gas engine, producing electricity and heat. The LT-CFB gasifier in the PolyGas system was air-blown.
b) SNG production plant: The gas from the PolyGas system was synthesized to SNG. Hydrogen was produced using alkaline electrolysis cells and mixed with the gas before synthesis, in order to maximize the SNG yield. The LT-CFB gasifier in the PolyGas system was oxygen-blown, using the oxygen from the electrolysis.
c) DME production plant: The gas from the PolyGas system was synthesized to DME. Hydrogen was produced using alkaline electrolysis cells and mixed with the gas before synthesis, in order to maximize the DME yield. The off-gas from the DME synthesis block was burned in a gas engine producing electricity

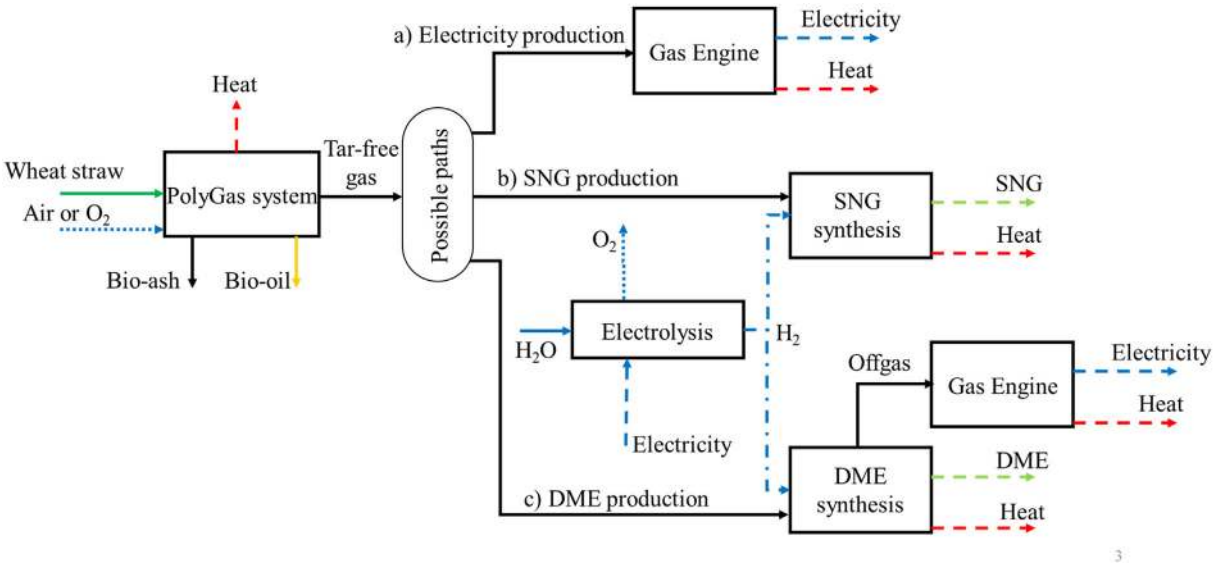

Fig. 3. Overview of the three plants investigated in this work: a) Electricity production plant, b) SNG production plant, c) DME production plant.

and heat. The LT-CFB gasifier in the PolyGas system was oxygen-blown, using the oxygen from the electrolysis.

Detailed flowsheets of the three investigated plants are shown in section S1 of the supplementary material.

In the following sections, the different blocks of the plants shown in Fig. 3 are described, including the modelling approaches. The numerical values of all design parameters are listed in Table 1. The plants were simulated using Aspen Plus V11 [20] with the property method RK-SOAVE (Redlich-Kwong-Soave) for all blocks, except the DME synthesis, where the property method SR-POLAR (Schwarzentruber and Renon) was used.

2.1. The PolyGas system

The PolyGas system consists of four main blocks, as shown in Fig. 2. In this work, the different components of the system were modelled and validated against experiments by Eschenbacher et al. [10]. The specific experiment, which was used for validation was conducted for a pyrolysis temperature of 662 °C and catalytic upgrading at 500 °C using γ-Al_2O_3 as catalyst.

2.1.1. Pyrolysis reactor of the LT-CFB gasifier

As shown in Fig. 1, the LT-CFB gasifier consists of a pyrolysis reactor, a char reactor and two cyclones. These components were modelled using a zero-dimensional approach, as proposed by Kaushal et al. [21]. The pyrolysis reactor was modelled by defining the composition and yield of char and tar. The gas composition was determined by fulfilling the elemental balances and assuming a balanced reaction, meaning neither exothermic nor endothermic [22–24]. The char composition and char yield were fixed according to experimental data of Trinh et al. [25]. The tar composition and tar yield (divided in bio-oil and aqueous organics) and the product ratio between the gaseous hydrocarbons were calculated according to experimental data [10] and fixed at the outlet of the pyrolysis reactor. A detailed description of the pyrolysis model is shown in section S2 of the supplementary materials.

The chemical energy content of char, bio-oil and aqueous organics was estimated using eq. (1) for the higher heating value of liquid and solid fuels [26].

$$\mathrm{HHV} = 0.3491\ \mathrm{C} + 1.1783\ \mathrm{H} + 0.1005\ \mathrm{S} - 0.1034\ \mathrm{O} - 0.0151\ \mathrm{N} - 0.0211\ \mathrm{A}\ \left[\frac{\mathrm{MJ}}{\mathrm{kg}}\right] \quad (1)$$

In Eq. (1), C, H, S, O, N and A denote the carbon, hydrogen, sulphur, oxygen, nitrogen and ash content in wt.-%, respectively.

The transport of the bed material between the pyrolysis and char reactor was not included in detail. It was modelled as a heat stream transferring the required heat for the pyrolysis reaction from the char reactor.

2.1.2. Char reactor of the LT-CFB gasifier

The char gasifier was modelled assuming chemical equilibrium at the outlet temperature and pressure. The temperature was defined and kept by fixing the heat loss to 1% of the chemical energy input of straw (LHV) and controlling the air/oxygen flow to the gasifier. Additionally, the amount of carbon left in the bio-ash was fixed to 10% of the carbon in the straw. This assumption achieved a reasonable fit between experimental and model gas composition of the mixture of gasification and pyrolysis gas.

2.1.3. Catalytic upgrading

For catalytic upgrading of the bio-oil, an adiabatic reactor was used. The catalytic reactor was modelled by defining composition and yield of bio-oil, aqueous organics and coke, formed on the catalyst. The gas composition was determined by fulfilling the elemental balances and defining the concentration of key components at the outlet of the catalytic reactor. Yield and composition of the upgraded bio-oil, aqueous organics and coke were calculated according to experimental data from Eschenbacher et al. [10]. Pentene and Benzene were assumed to be the only gaseous compounds to react on the catalyst. Changes in the gas composition were assumed to occur only for propene, pentene, benzene, carbon dioxide and steam. A detailed description of the catalytic upgrading model is shown in section S3 of the supplementary materials.

2.1.4. Catalyst regeneration

The coke formed on the catalyst needs to be combusted in order to regenerate the catalysts. Technically, there are two ways of realizing this. First, a circulating fluid bed can be used, where the catalyst is circulating between the bio-oil upgrading reactor and the regeneration reactor. The second alternative is to use several fixed bed reactors in parallel. In a batch process, one reactor is used for upgrading bio-oil, while the catalyst in the other reactor or several other reactors is regenerated. In this work, the regeneration was modelled as a coke stream flowing to a combustion reactor, where it was combusted using diluted air. Compressed fresh air was diluted by recycling parts of the exhaust gas from the catalyst regenerator. This is required in order to avoid an excessive temperature increase that could damage the catalyst during regeneration. Inlet and outlet oxygen concentration of the coke combustion were fixed in order to ensure complete combustion while avoiding hot spots in the reactor. The recycling stream was cooled additionally in order to control the combustion temperature.

2.1.5. Bio-oil collector

After the catalytic reactor, the gas was cooled to ambient temperature and the bio-oil and aqueous organics condensed. Experiments showed that the two liquid phases could be separated easily. The aqueous organics were disposed, as an extraction of the organics from the water phase seemed unfeasible.

2.2. Water electrolysis

Alkaline water electrolysis was used to produce hydrogen for the SNG and the DME production plant. The electrolysis was modelled by defining a conversion efficiency for the production of hydrogen. A lower heating value (LHV) efficiency from electricity to hydrogen of 70% was used [27,28]. The rest of the electricity input in the electrolysis is released as heat. The operating temperature of the electrolysis plant was at 90 °C, enabling provision of district heating. The operating pressure was chosen to match the mixing pressure of the hydrogen with the gas (10.8 bar for SNG and 46.1 bar for DME production), reducing the electricity consumption needed for hydrogen compression.

2.3. Gas engine

In the electricity production and the DME production plant, a gas engine with compressed air was used for combusting the gas and the off-gas from DME synthesis, respectively. The operation of a gas engine on syngas is described in Ref. [29].

2.4. SNG synthesis

For SNG synthesis, the gas was compressed to 10.8 bar and mixed with the electrolytic hydrogen. The amount of hydrogen needed for an optimal methane synthesis depends on the gas composition. For methane synthesis, a module M = 3 (eq. (2)) is

Table 1
Process design parameter.

Biomass feed (Straw)				
The biomass input was assumed at 50 MWth (LHV dry)				
Moisture: 8.5 wt%, ash; 6.6 wt%, composition (daf) [wt%]: N 0.8; C 46.2; H 6.6; O 46.4				[10]
	HHV[a] = 26.1 MJ/kg_{dry}	c_p = 1.35 kJ/(kg_{dry}*K)		[32]
Pyrolysis reactor				
	$T_{Pyrolysis}$ = 660 °C	$\Delta p_{Pyrolysis}$ = 0.15 bar		
The pyrolysis reaction was modelled assuming LHV balance and fixing the following output parameters:				
Char:	Composition (daf) [wt%]:	N 1.4; C 67.2; H 4.5; O 26.9		[25]
	Ash content char (dry) [wt%]:	21.1		[25]
	HHV[a] = 20.0 MJ/kg_{dry}	c_p = 1.15 kJ/(kg_{dry}*K)		[32]
Bio-oil	Composition [wt %]:	N 3.7; C 74.8; H 7.2; O 14.3		[10]
	Yield based on dry straw [wt %]:	10.33		[10]
	HHV[a] = 33.1 MJ/kg_{dry}	c_p = 3 kJ/(kg_{dry}*K)		[33]
Aq. Organics	Composition [wt %]:	N 11.5; C 46.2; H 11.3; O 31.0		[10]
	Yield based on dry straw [wt %]:	3.17		[10]
	HHV[a] = 26.1 MJ/kg_{dry}	c_p = 3 kJ/(kg_{dry}*K)		[33]
Pyrolysis gas[b]	x_{C2H6}/x_{CH4} = 0.187	x_{C2H4}/x_{CH4} = 0.425	x_{C3H6}/x_{CH4} = 0.28	
	x_{C5H10}/x_{CH4} = 0.085	x_{C6H6}/x_{CH4} = 0.021	x_{H2} = 0	
Char gasifier				
	$T_{Gasification}$ = 730 °C	$\Delta p_{Gasification}$ = 0.15 bar		
Chemical equilibrium assumed at the outlet temperature and pressure.				
Ash	Carbon conversion [%]:.	90	No N, H and O remaining in ash.	
	HHV[a] = 7.6 MJ/kg_{dry}		c_p = 1.15 kJ/(kg_{dry}*K)	[32]
Catalytic upgrading				
	T_{Inlet} = 500 °C	$\Delta p_{Cataysis}$ = 0.15 bar		
Catalytic upgrading was assumed to be adiabatic with no heat loss.				
Coke	Composition [wt %]:	C 90; H 10.		[10]
	Yield based on tar input [wt %]:	23.2		[10]
	HHV[a] = 43.2 MJ/kg_{dry}	c_p = 1.15 kJ/(kg_{dry}*K)		[32]
Bio-oil	Composition [wt %]:	N 4.5; C 76.6; H 8.1; O 10.8		[10]
	Yield based on tar input [wt %]:	52		[10]
	HHV[a] = 25.1 MJ/kg_{dry}	c_p = 3 kJ/(kg_{dry}*K)		[33]
Aq. Organics	Composition [wt %]:	N 22.1; C 42.7; H 12.4; O 22.8		[10]
	Yield based on tar input [wt %]:	14.3		[10]
	HHV[a] = 26.8 MJ/kg_{dry}	c_p = 3 kJ/(kg_{dry}*K)		[33]
Gas yields	$\dot{n}_{C3H6,Outlet}/\dot{n}_{C3H6,Inlet}$ = 1.34	$\dot{n}_{C5H10,Outlet}/\dot{n}_{C6H6,Outlet}$ = 15		
	$\dot{n}_{H2,Outlet}/\dot{n}_{H2,Inlet}$ = 1	$x_{O2,Outlet}$ = 0		
Coke combustion				
T_{outlet} = 700 °C	$x_{O2,Inlet}$ = 3 wt%	$x_{O2,Outlet}$ = 1 wt%	$\Delta p_{Coke\ combustion}$ = 0.15 bar	
Bio-oil condensation				
$T_{Condensation}$ = 25 °C	$x_{H2O,\ Bio\text{-}oil}$ = 2.5 wt%	$\Delta p_{Bio\text{-}oil\ Collctor}$ = 0.01 bar		
Water electrolysis				
	$T_{Electrolysis}$ = 90 °C	Energy efficiency (LHV) = 70% (electricity to hydrogen).		
Gas engine				
$T_{Exhaust}$ = 400 °C	Excess air ration (λ) = 2	p_{Inlet} = 2 bar		
Energy efficiency (LHV) = 38% (gas to electricity).				
SNG synthesis				
Boiling water reactor (isothermal). Chemical equilibrium assumed at the outlet temperature and pressure.				
C2+ hydrocarbons were assumed as inert during synthesis.				
$T_{SNG\ synthesis}$ = 280 °C	p_{Inlet} = 10.7 bar	$\Delta p_{SNG\ Synthesis}$ = 0.7 bar		
Module M = 3 (eq. (6))				
DME synthesis				
Boiling water reactor (isothermal). Temperature approach was assumed for chemical equilibrium.				
The approach temperature differences used were: 15 °C (eq. (9)), 100 °C (eq. (10)), 15 °C (eq. (11)) [18].				
$T_{DME\ synthesis}$ = 240 °C	p_{Inlet} = 46 bar	$\Delta p_{DME\ Synthesis}$ = 0.7 bar.		
Distillation				
Topping column (TC): 30 stages; feed stage: 15.				
p_{TC} = 9 bar	$\dot{n}_{C3H6,Top}/\dot{n}_{C3H6,feed}$ = 0.999	$\dot{n}_{DME,Bottom}/\dot{n}_{DME,feed}$ = 0.999		
DME column (DC): 20 stages; feed stage: 14.				
p_{DC} = 6.8 bar	$y_{DME,Top}$ = 99.99 mol%	$\dot{n}_{C5H10,Top}/\dot{n}_{C5H10,feed}$ = 0.9999		
Cooling				
COP = 1.2				
Heat exchangers				
$\Delta T_{gas\text{-}air/oxygen}$ = 100 K	$\Delta T_{gas\text{-}gas}$ = 30 K	$\Delta T_{gas\text{-}liq}$ = 10 K		
$\Delta p_{HEX,\ ambient}$ = 0.01 bar[c]	$\Delta p_{HEX,\ intermediate}$ = 0.1 bar[d]			
Process heat				
$T_{Process\ heat}$ = 200 °C	Process heat supply quality = 1.	Process heat return quality = 0.		

(*continued on next page*)

Table 1 (*continued*)

District heating	
$T_{\text{District heating, supply}} = 75\ ^\circ\text{C}$	$T_{\text{District heating, return}} = 40\ ^\circ\text{C}$
Turbomachinery	
$\eta_{\text{Polytropic}} = 0.8$.	$\eta_{\text{Mechanical}} = 0.94$.
In the DME synthesis, 5-stage gas compression with intercooling to 50 °C and constant pressure ratio across each compressor was used.	

[a] Calculated using eq. (1).
[b] All component ratios are on mass basis and are derived from experimental results in Ref. [10].
[c] Heat exchangers operating at pressures p < 2 bar are defined as operating at ambient pressures.
[d] Heat exchangers operating at pressures 50 bar > p ≥ 2 bar are defined as operating at intermediate pressures.

needed in order to maximize the methane yield. The module can be derived from the methanation reactions shown in eqs. (3) and (4).

$$M = \frac{H_2 - CO_2}{CO + CO_2} \tag{2}$$

$$CO + 3\,H_2 \leftrightarrow CH_4 + H_2O \quad -206\ \text{kJ/mol} \tag{3}$$

$$CO_2 + 4\,H_2 \leftrightarrow CH_4 + 2\,H_2O \quad -165\ \text{kJ/mol} \tag{4}$$

After preheating the gas/hydrogen mixture, it was led to the boiling water reactor, where the methanation reactions occurred. In accordance with [30], the gas at the outlet of the reactor was assumed to be at chemical equilibrium at the outlet temperature (280 °C) and pressure. The produced gas was cooled to ambient temperature and water was removed through condensation and a water removal system. The dry SNG could then be injected to the gas grid or liquefied and used for other purposes.

2.5. DME synthesis

The DME synthesis block was designed with one-stage DME synthesis with recycling of unconverted gas back to the DME reactor as proposed in the DME RC-plants in Refs. [17,18]. The gas was compressed to 46.1 bar using a 5-stage compression with intercooling, before mixing it with hydrogen. The gas mixture was led to a boiling water reactor operating at 240 °C. The reactions occurring during DME synthesis are methanol synthesis (eq. (5)), methanol dehydration (eq. (6)) and water gas shift reaction (eq. (7)). These three reactions can be summarized to the net DME synthesis reaction shown in eq. (8). Eq. (8) shows that the optimal H_2/CO ratio for one-step DME synthesis equals one. However, providing hydrogen for this ratio would lead to an external oxygen demand for the LT-CFB gasifier, as there was not enough oxygen produced during electrolysis. Hence, the electrolysis was designed to fulfill the oxygen demand for the gasification unit and a higher H_2/CO ratio (1.2) was accepted.

$$4\,H_2 + 2\,CO \leftrightarrow 2\,CH_3OH \quad -182\ \text{kJ/mol} \tag{5}$$

$$2\,CH_3OH \leftrightarrow CH_3OCH_3 + H_2O \quad -23\ \text{kJ/mol} \tag{6}$$

$$CO + H_2O \leftrightarrow CO_2 + H_2 \quad -41\ \text{kJ/mol} \tag{7}$$

$$3\,H_2 + 3\,CO \leftrightarrow CH_3OCH_3 + CO_2 \quad -246\ \text{kJ/mol} \tag{8}$$

After the synthesis reactor, the product stream was cooled to −50 °C before the gas-liquid separator. 95% of the gas was recycled to the DME reactor. The remaining 5% was sent to the gas engine. This was required in order to avoid accumulation of inerts (N_2, CH4, C2H6 etc.) in the synthesis loop. The liquid stream from the separator was sent to the topping column, where the components lighter than DME were separated and then combusted in the gas engine. The bottom product was purified in the DME column, yielding a DME stream with a purity of 99.99%. The bottom stream was sent to the gas engine.

2.6. District heating and process heat

All three plants based on the PolyGas system can provide surplus heat at different temperature levels. As highlighted by Bühler et al. [31], the largest share of the heat demand of the industry sector in Denmark is found at temperatures above 150 °C. At the same time, reducing the use of fossil fuels for providing high temperature heat is significantly more difficult than for lower temperatures. This makes it interesting to investigate, whether biofuel production plants can provide heat at high temperatures. To do so, the heat output of the three plants was divided into three different parts. Heat at temperatures high enough to provide saturated steam at 200 °C was defined as process heat. Heat at temperatures high enough to heat water from 40 °C to 75 °C was defined as district heating. Heat at lower temperatures was considered as heat loss. This low-temperature heat could be used as heat source for heat pumps providing district heating. This was however outside the scope of this study.

2.7. Evaluation criteria

The presented plants were compared to each other using the energy efficiency and the carbon efficiency. Two different energy efficiencies were calculated. The first energy efficiency η_{main} (eq. (9)) included the main products of the plants, which were the bio-oil output and electricity, SNG or DME for the three different polygeneration plants, respectively. The overall energy efficiency η_{tot} (eq. (10)) additionally accounted for the provided process heat and district heating. The term $\dot{W}_{net,out}$ in eq. (9) and eq. (10) denotes the net power output and was considered only for the electricity production plant, while $\dot{W}_{net,in}$ denotes the net power input, which was considered for the SNG and the DME production plant.

$$\eta_{\text{main}} = \frac{\dot{m}_{Bio-oil} \cdot LHV_{Bio-oil} + \dot{m}_{Electrofuel} \cdot LHV_{Electrofuel} + \dot{W}_{net,out}}{\dot{m}_{Straw} \cdot LHV_{Straw} + \left|\dot{W}_{net,in}\right|} \tag{9}$$

$$\eta_{tot} = \frac{\dot{m}_{Bio-oil} \cdot LHV_{Bio-oil} + \dot{m}_{Electrofuel} \cdot LHV_{Electrofuel} + \dot{W}_{net,out} + \dot{Q}_{PH} + \dot{Q}_{DH}}{\dot{m}_{Straw} \cdot LHV_{Straw} + \left|\dot{W}_{net,in}\right|} \quad (10)$$

In order to evaluate, how much of the carbon in the straw input to the plants is converted, two carbon efficiencies were defined. The first carbon efficiency γ_{main} (eq. (11)) included the carbon bound in the transport fuels produced in the plants, namely bio-oil and electrofuels (SNG or DME). The overall carbon efficiency γ_{tot} (eq. (12)) included also the carbon bound in the bio-ashes which could be sequestrated in the soil by returning the bio-ashes to the wheat fields.

$$\gamma_{main} = \frac{\dot{m}_{C,Bio-oil} + \dot{m}_{C,Electrofuel}}{\dot{m}_{C,Straw}} \quad (11)$$

$$\gamma_{tot} = \frac{\dot{m}_{C,Bio-oil} + \dot{m}_{C,Electrofuel} + \dot{m}_{C,Bio-ash}}{\dot{m}_{C,Straw}} \quad (12)$$

3. Results

The results are divided into three subsections, one for each plant, followed by a comparison of the plants. Detailed results of the simulations, including thermodynamic data and compositions of the different streams are in section S1 of the supplementary materials. In order to evaluate the energetic performance of the investigated plants, the energy flows entering and exiting the plant and the different conversion blocks (Fig. 3) were examined. Additionally, the carbon flows into and out of the plants and conversion blocks were investigated to evaluate the conversion of the carbon in straw to carbon bound in bio-ash or transport fuels.

3.1. Electricity production plant

Fig. 4 shows the energy flows in the electricity production plant. It shows that the PolyGas system converted straw into four parts: gas, liquids, ash and heat. The chemical energy in the gas is the biggest part of the products, corresponding to 54% of the chemical energy in the straw. The liquid phase was separated into two parts, bio-oil and aqueous organics. Bio-oil was one of the main products of the plant, yielding a chemical energy recovery of 14% of the straw input. The energy of the aqueous organics was regarded as an energy loss. The bio-ash, which was returned to the wheat field, had a carbon content of 37.3 wt%. This lead to an energy loss of 8%. The rest of the chemical energy in the straw was released as heat. Together with the heat produced in the gas engine, process heat and district heating corresponding to 40% and 12% of the straw input were produced, respectively. The heat loss of 2% consisted of the heat loss of the gasifier and the cooling of the gas to 25 °C in the bio-oil collector for condensation.

After condensing the bio-oil and the aqueous organics, the tar-free gas was combusted in a gas engine producing electricity and heat. From Fig. 4, it can be seen that 19% of the chemical energy in the straw ends up as electricity. This denotes the net electricity production of the plant. Parts of the electricity produced in the gas engine was used for providing air to the LT-CFB gasifier and the catalyst regeneration (shown in the recycling stream) and for the air compressor of the gas engine (not shown in Fig. 4).

Fig. 5 depicts the carbon flows in the electricity production plant. 10% of the carbon in the straw were bound in the bio-ash and returned to the wheat field. Through pyrolysis and gasification, the carbon is fixed in the bio-ash and hence stored in the soil. The bio-oil contained 13% of the carbon, making it available for later use as fuel or chemical base material. Carbon was lost in the PolyGas system in form of aqueous organics (2%) and CO_2 released through combustion of the coke in the catalyst regeneration (7%). 69% of the

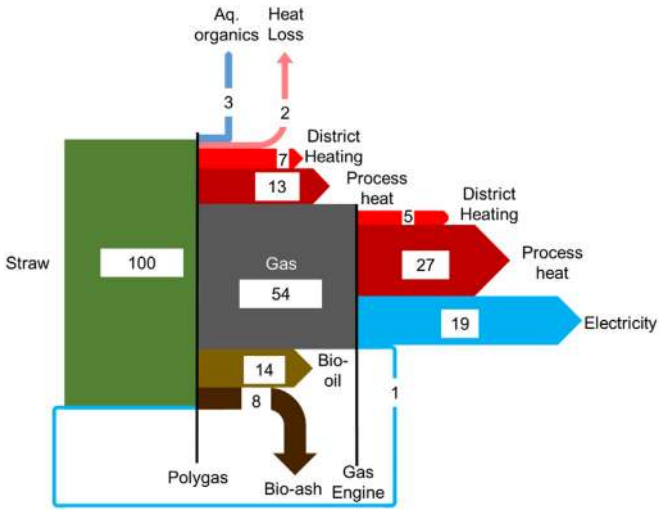

Fig. 4. Electrical, heat and chemical energy (LHV) flows for the electricity production plant. Note: All flows are normalized to the chemical energy input of straw. The numbers denote the normalized percentage of the respective energy flow.

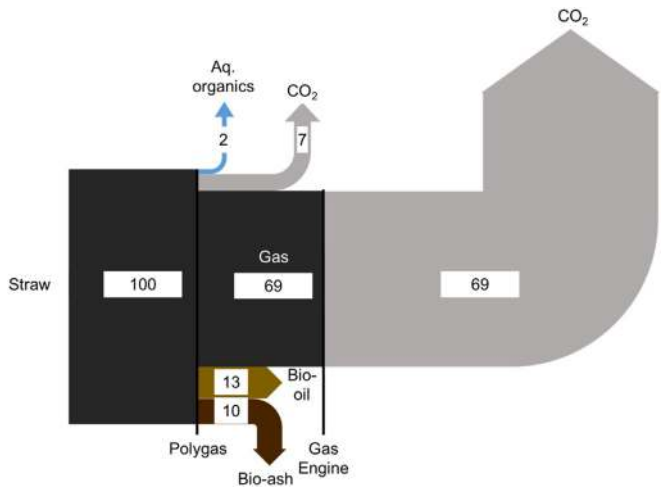

Fig. 5. Carbon flows for the electricity production plant. Note: All flows are normalized to the carbon input of straw. The numbers denote the normalized percentage of the respective carbon flow.

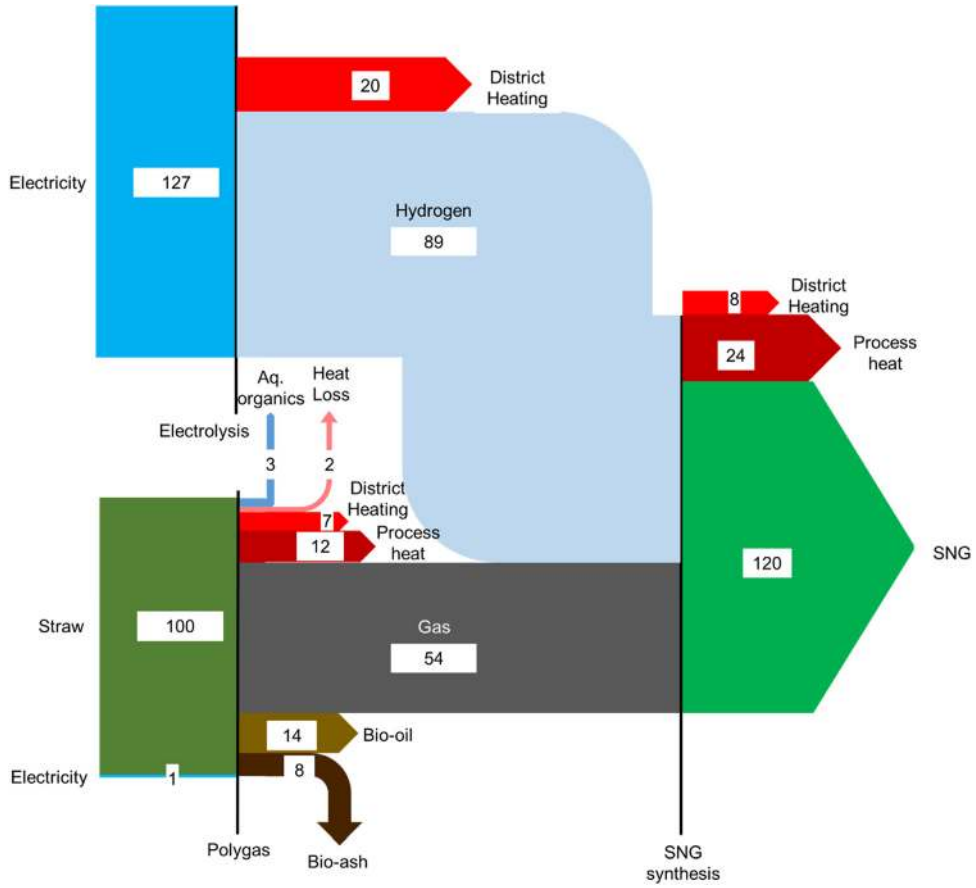

Fig. 6. Electrical, heat and chemical energy (LHV) flows for the SNG production plant. Note: All flows are normalized to the chemical energy input of straw. The numbers denote the normalized percentage of the respective energy flow.

carbon ended up in the gas, which was combusted in the gas engine. Thereby, the carbon was converted to CO_2 and released to the environment.

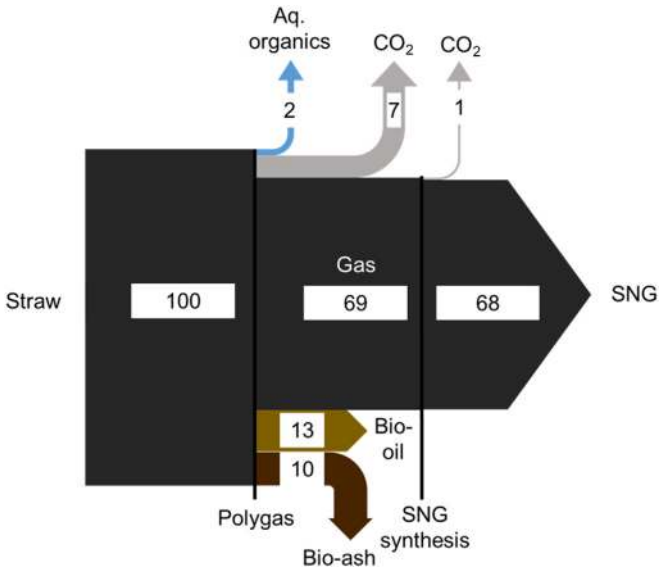

Fig. 7. Carbon flows for the SNG production plant. Note: All flows are normalized to the carbon input of straw. The numbers denote the normalized percentage of the respective carbon flow.

3.2. SNG production plant

Fig. 6 shows the energy flows in the SNG production system. The results for the PolyGas system were similar to the results showed in the previous section. However, the absolute values of the chemical energy flow of the gas and the district heating output are slightly different due to the oxygen-blown operation of the LT-CFB gasifier. The most significant difference to the electricity production case is the reduced process heat output in the SNG production plant, caused by preheating the oxygen from the electrolysis cell using heat from the exhaust gas of the catalyst regeneration. The oxygen was then expanded in a turbine generating electricity for internal use.

The net electricity consumption of the SNG production plant is 128% of the straw input. The major part of this electricity (127%) was consumed by the electrolysis plant producing the amount of hydrogen needed for converting CO and CO_2 to methane. The electrolysis plant produced hydrogen with a chemical energy flow of 89% of the straw input. Operating the electrolysis at 90 °C enabled to recover heat for district heating, corresponding to 20% of the straw input.

Using the produced hydrogen, a chemical energy flow of SNG corresponding to 120% of the straw input was obtained. The synthesis efficiency of hydrogen and gas to SNG was 83.5%. By cooling the methanation reactor with boiling water, process heat corresponding to 24% of the straw input was generated. By cooling the SNG stream, 8% of the chemical energy in the straw were recovered for district heating.

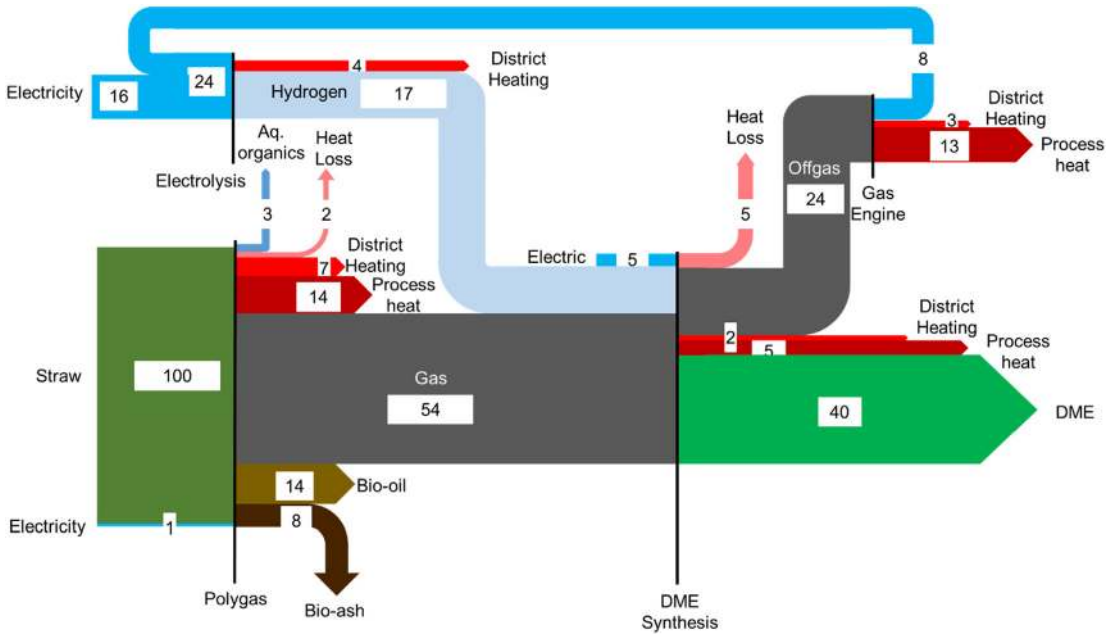

Fig. 8. Electrical, heat and chemical energy (LHV) flows for the DME production plant. Note: All flows are normalized to the chemical energy input of straw. The numbers denote the normalized percentage of the respective energy flow.

The carbon flows in the SNG production plant are shown in Fig. 7. There are no differences in carbon flows for the PolyGas system compared to the electricity production plant. However, the conversion of gas to SNG avoided the emission of 69% of the carbon as CO_2 and enabled instead to bind 68% of the carbon as hydrocarbons in SNG. 1% of the carbon exited the plant as CO_2 in the SNG.

3.3. DME production plant

The energy flows of the DME production plant are shown in Fig. 8. The results for the PolyGas system were similar to the electricity production and the SNG production plant. The process heat output was however slightly higher, even though preheating of the oxygen before the oxygen turbine and the gasifier was included. This was caused by a lower oxygen mass flow from the electrolysis plant due to the lower hydrogen requirement.

The chemical energy content of the produced hydrogen corresponded to 17% of the straw input. The electrolysis cell was operated according to the oxygen demand of the LT-CFB gasifier. Therefore, the H_2/CO ratio at the DME reactor inlet was 1.2 instead of the ideal value of 1 for DME synthesis.

In the DME synthesis block, electricity corresponding to 5% of the straw input was used for gas compression and for condensation in the topping column at −45 °C. The chemical energy output in form of DME corresponded to 40% of the straw input, while 5% of the chemical energy of the straw was recovered as process heat. The process heat derived from the DME synthesis reactor. However, 29% of the high temperature heat was used within the DME synthesis block for preheating streams and as heat source for the reboilers of the distillation columns. 2% of the straw input was recovered for district heating by intercooling in the 5-stage

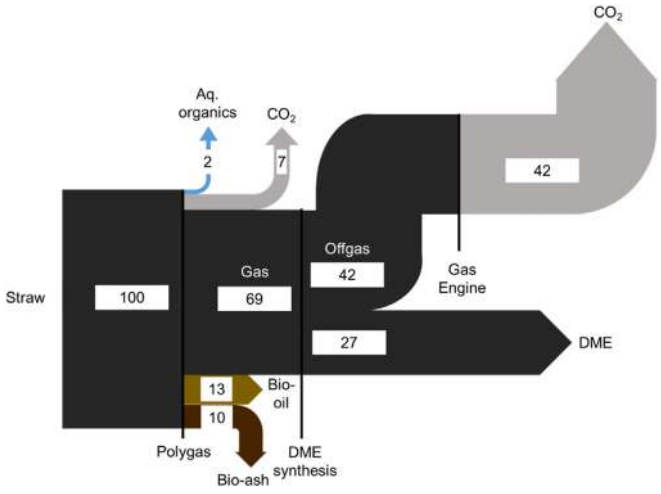

Fig. 9. Carbon flows for the DME production plant. Note: All flows are normalized to the carbon input of straw. The numbers denote the normalized percentage of the respective carbon flow.

Table 2
Summary of energy and carbon inputs and products of the three biorefineries. Note. All chemical energy flows are based on LHV.

	Electricity production		SNG production		DME production	
	Energy [MW]	Carbon [kg/h]	Energy [MW]	Carbon [kg/h]	Energy [MW]	Carbon [kg/h]
Inputs						
Straw	50.00	4760	50.00	4760	50.00	4760
Net electricity	–	–	64.19	–	10.83	–
Main products						
Bio-oil	7.21	596	7.21	596	7.21	596
Net electricity	9.23	–	–	–	–	–
SNG	–	–	59.85	3251	–	–
DME	–	–	–	–	19.76	1287
Byproducts						
Process heat	20.05	–	17.87	–	15.84	–
District heating	6.36	–	17.37	–	7.51	–
Bio-ash[a]	–	476	–	476	–	476

[a] The chemical energy content of bio-ash is not listed, as it is not a useful product of the plants.

Table 3
Energy and carbon efficiencies of the three biorefineries.

	Electricity production		SNG production		DME production	
	Energy (LHV) Efficiency	Carbon Efficiency	Energy (LHV) Efficiency	Carbon Efficiency	Energy (LHV) Efficiency	Carbon Efficiency
	[%]	[%]	[%]	[%]	[%]	[%]
Main products	33	13	59	81	44	40
All products	86	23	90	91	83	50

compression of the gas. The heat loss in the DME synthesis block accounted for 5% of the chemical energy of the straw. It was caused by cooling down streams below the district heating temperature and by heat released at the condensers of the refrigeration systems.

The off-gas from the DME synthesis block had a chemical energy content corresponding to 24% of the straw input. This was caused by inert hydrocarbons in the gas. Additionally, heavy hydrocarbons (Pentene and Benzene) in the bottom stream of the DME column inhibited the possibility of recycling methanol to the synthesis reactor and further increasing the DME yield. The off-gas was combusted in the gas engine, producing electricity (8%), process heat (13%) and district heating (3%). By using the electricity produced in the gas engine for electrolysis, the net electricity consumption of the electrolysis plant was reduced to 16% of the straw input. The net electricity consumption of the DME production plant corresponded to 22% of the straw input.

Fig. 9 depicts the carbon flows in the DME production plant. The carbon inflows and outflows of the PolyGas system are equal to the electricity and the SNG production plant. Through the DME synthesis block, 27% of the carbon in the straw ended up in the DME and 42% in the off-gas. Approx. 2/3 of the carbon in the off-gas was in the form of CO_2, while approx. 1/3 was in the form of hydrocarbons. The off-gas was then combusted in the gas engine, emitting all the carbon as CO_2 (42%).

3.4. Comparison of the biorefineries

The three investigated biorefinery plants where compared for their energy and carbon efficiency, as shown in section 2.7. Table 2 lists the energy and carbon inputs and products of each plant. Table 3 shows the calculated energy and carbon efficiencies. In both tables, the products were divided into main products and byproducts. The main products included the produced fuels and the net electricity production. Process heat and district heating were byproducts considered in the energy analysis. Bio-ash was considered as byproduct for the carbon conversion performance.

The SNG production system achieved the highest values for all carbon efficiencies (81% including the main products, 91% including all products) and energy efficiencies (59% including the main products, 90% including all products). The SNG production plant converted nearly all CO and CO_2 in the gas to CH_4 in the SNG. This was achieved by using 64 MW of net electricity, which is almost six times more than for the DME production plant. The DME production plant yielded the lowest overall energy efficiency for the investigated plants (83%), while the energy efficiency considering only the main products, DME and bio-oil, was higher than for the electricity production plant. The lower overall energy efficiency was caused by heat losses in the DME synthesis block and increased internal high-temperature heat demand for the distillation columns. The district heating production was however higher than for the electricity production plant. The SNG production plant provided most district heating, while the electricity production plant produced the highest amount of process heat. The electricity production plant achieved an overall energy efficiency of 86%. However, more than 50% of the energy input was converted to heat, while only 33% ended in the main products, bio-oil and electricity. Additionally, combustion of the gas lead to a low carbon efficiency of 22.5%, including the carbon in the bio-ash.

4. Discussion

This study was conducted using newly built components for the pyrolysis unit of the LT-CFB gasifier and the catalytic reactor for upgrading of bio-oil. The model was based on a single experiment conducted at the temperatures and with the catalyst as described. The measurement uncertainties together with the additional assumptions for the pyrolysis and the catalytic upgrading induced uncertainties in the outputs of these components, such as the exact tar yields and the gas compositions. More experiments conducted under the same conditions are required for increasing the fidelity of the model. Additionally, investigating the influence of varying the pyrolysis temperatures on the bio-oil yield would be interesting. However, no experimental data of the LT-CFB gasifier together with γ-Al_2O_3 as catalyst were available. This made it impossible to predict the behavior at different pyrolysis conditions.

The comparison of three different biorefineries showed that the SNG production plant yielded the highest carbon efficiency and energy efficiency. The plant benefited from the high amount of methane and higher gaseous hydrocarbons in the gas, which were not necessary to convert. For the DME production plant on the other hand, the presence of the hydrocarbons hindered the possibility of achieving high carbon efficiencies, as the investigated plant design did not enable the conversion of the hydrocarbons. The addition of a partial oxidation step could increase the carbon efficiency of the DME production plant and should be further investigated. This would however further increase the plant complexity and the influence on the economy should be considered. When comparing the SNG and DME production plant, it should be considered that the fuel properties of DME are significantly favorable compared to SNG [16]. This difference was not included in this analysis. A well-to-wheel efficiency, describing the efficiency from wheat straw to the movement of vehicles (ships, trucks, etc.) should be determined in order to have a fair comparison between the two production plants.

In this work, alkaline water electrolysis was used for producing hydrogen and oxygen. Different studies have shown the possibility of achieving high energy efficiency (up to 84% for main products) biofuel systems through steam electrolysis [11,22] or co-electrolysis [13,15] with solid oxide cells. The results showed that both electrofuel producing plants had available surplus heat which could be used for providing steam for solid oxide electrolysis. This could further increase the energy efficiency by reducing the net electricity consumption.

The electricity production plant achieved a good overall energy efficiency. However, the analysis of the carbon efficiencies showed that only 22.5% of the valuable carbon in the straw were bound in form of bio-oil and in the bio-ash. The electricity production would in a future 100% renewable energy system be in competition to

other back up power generation units, i.e. biogas based gas engines or electricity storage systems. The decisive factor in this competition will be the price of the provided electricity. It can be expected that the electricity production plant presented in this in this work would suffer from its comparably high investment costs. A way to counteract the high investment cost would be to increase the operation time of the system. In a smart energy system context, it would make sense to combine the electricity production plant with one of the fuel production plants in one combined plant. Such a system could produce backup power when renewable power from wind and solar is insufficient and produce electrofuels when there is surplus electricity. This would increase the operation time of the system and lead to high carbon efficiencies compared to electricity production only. Such flexible systems have been investigated in Refs. [23,34].

All the proposed plants produced more than 15 MW_{th} of process heat from 50 MW_{th} of straw. By locating the biorefineries nearby industrial facilities, an efficient use of the high temperature heat could be achieved. It should also be noted that even though process heat was defined as the provision of steam at 200 °C, provision of temperatures up to 700 °C would be possible by adequate integration between the industrial processes and the biorefinery plant. The same accounts for the provision of district heat. However, the amount of provided district heating was lower than for process heat (except for the SNG production plant).

5. Conclusion

In this work, three novel polygeneration plants based on wheat straw gasification using the low-temperature circulating fluidized bed (LT-CFB) gasifier followed by a catalytic reactor for deoxygenating the tars in the gas were investigated. The work aimed to assess the performance of the polygeneration systems integrating the electricity, heating and transport sector and hence being potentially important actors in a Smart Energy System. The performance was evaluated through their energy and carbon efficiencies. The three investigated plants were:

- The electricity production plant, producing bio-oil and electricity
- The synthetic natural gas (SNG) production plant, producing bio-oil and SNG, while using electricity for producing electrolytic hydrogen
- The dimethyl ether (DME) production plant, production bio-oil and DME, while using electricity for producing electrolytic hydrogen

Overall, this work showed that wheat straw based polygeneration plants can play an important role in a future smart energy system, as they enable an efficient conversion of residual biomass to transport fuel, process heat, district heating and electricity, where applicable. The results showed that the SNG production plant performed best in terms of energy and carbon efficiency. The analysis of the DME production plant showed high energy efficiency, however, the proposed plant design did not reach an optimal carbon conversion. Further improvements in the plant design could enable higher carbon efficiencies, yielding more DME, which is the most promising transport fuel investigated in this study. The electricity production plant yielded the lowest carbon efficiency of the investigated plants. However, compared to other, more established biomass-based electricity production plants like biogas- or wood-based CHP plants, the carbon efficiency is significantly higher due to the possibility of carbon sequestration in the bio-ash and producing bio-oil.

Declaration of competing interest

The authors declare that they have no known competing financial interests or personal relationships that could have appeared to influence the work reported in this paper.

Acknowledgments

This research project was financially funded by ForskEL/EUDP under the project “PolyGas – Polygeneration of bio-oil, electricity, heat and bioashes from thermal gasification of biomass and waste” (project identification: ForskEL – 12454). The provision of detailed experimental data by Andreas Eschenbacher and his help are gratefully acknowledged.

Appendix A. Supplementary data

Supplementary data to this article can be found online at https://doi.org/10.1016/j.segy.2021.100015.

Nomenclature

A	Ash content, wt%
C	Carbon content, wt%
COP	Coefficient of performance,
c_p	Specific heat capacity, kJ/(kg*K)
H	Hydrogen content, wt%
HHV	Higher heating value, MJ/kg
LHV	Lower heating value, MJ/kg
M	Gas module,
$\dot{m}$	Mass flow rate, kg/s
N	Nitrogen content, wt%
$\dot{n}$	Molar flow rate, mole/s
O	Oxygen content, wt%
p, Δp	Pressure, pressure drop, bar
S	Sulphur content, wt%
T	Temperature, °C
$\dot{W}$	Power, MW
x	Mass fraction, wt%
y	Molar fraction, mole%

Greek symbols

γ	Carbon efficiency, %
η	Energy efficiency, %
$\eta_{Mechanical}$	Mechanical efficiency,
$\eta_{Polytropic}$	Polytropic efficiency,

Subscripts and superscripts

C	Carbon
DC	DME column
DH	District heating
main	Main products
PH	Process heat
tot	Total
TC	Topping column

Abbreviations

Aq	Aqueous
daf	Dry and ash-free
DME	Dimethyl ether
LHV	Lower heating value
LT-CFB	Low temperature circulating fluidized bed
SNG	Synthetic natural gas

References

[1] Lund H, Østergaard PA, Connolly D, Mathiesen BV. Smart energy and smart energy systems. Energy 2017;137:556–65. https://doi.org/10.1016/j.energy.2017.05.123.

[2] Mathiesen BV, Lund H, Connolly D, Wenzel H, Ostergaard PA, Möller B, et al. Smart Energy Systems for coherent 100% renewable energy and transport solutions. Appl Energy 2015;145:139–54. https://doi.org/10.1016/j.apenergy.2015.01.075.

[3] Eickhout B, van den Born GJ, Notenboom J, van Oorschot M, Ros JPM, van Vuuren DP, et al. Local and global consequences of the EU renewable directive for biofuels: testing the sustainability criteria. 2008.

[4] Venturini G, Pizarro-Alonso A, Münster M. How to maximise the value of residual biomass resources: the case of straw in Denmark. Appl Energy 2019;250:369–88. https://doi.org/10.1016/j.apenergy.2019.04.166.

[5] Ahrenfeldt J, Thomsen TP, Henriksen U, Clausen LR. Biomass gasification cogeneration - a review of state of the art technology and near future perspectives. Appl Therm Eng 2013;50:1407–17. https://doi.org/10.1016/j.applthermaleng.2011.12.040.

[6] Hansen V, Müller-Stöver D, Ahrenfeldt J, Holm JK, Henriksen UB, Hauggaard-Nielsen H. Gasification biochar as a valuable by-product for carbon sequestration and soil amendment. Biomass Bioenergy 2015;72:300–8. https://doi.org/10.1016/j.biombioe.2014.10.013.

[7] Sigurjonsson HÆ, Elmegaard B, Clausen LR, Ahrenfeldt J. Climate effect of an integrated wheat production and bioenergy system with Low Temperature Circulating Fluidized Bed gasifier. Appl Energy 2015;160:511–20. https://doi.org/10.1016/j.apenergy.2015.08.114.

[8] Thomsen TP, Sárossy Z, Gøbel B, Stoholm P, Ahrenfeldt J, Jappe Frandsen F, et al. Low temperature circulating fluidized bed gasification and co-gasification of municipal sewage sludge . Part 1 : process performance and gas product characterization. Waste Manag 2017;66:123–33. https://doi.org/10.1016/j.wasman.2017.04.028.

[9] Eschenbacher A, Jensen PA, Henriksen UB, Ahrenfeldt J, Li C, Duus JØ, et al. Deoxygenation of wheat straw fast pyrolysis vapors using HZSM-5, Al2O3, HZSM-5/Al2O3 extrudates, and desilicated HZSM-5/Al2O3 extrudates. Energy Fuels 2019;33:6405–20. https://doi.org/10.1021/acs.energyfuels.9b00906.

[10] Eschenbacher A, Jensen PA, Henriksen UB, Ahrenfeldt J, Jensen CD, Li C, et al. Catalytic upgrading of tars generated in a 100 kW th low temperature circulating fluidized bed gasifier for production of liquid bio-fuels in a polygeneration scheme. Energy Convers Manag 2020;207. https://doi.org/10.1016/j.enconman.2020.112538.

[11] Clausen LR. Energy efficient thermochemical conversion of very wet biomass to biofuels by integration of steam drying , steam electrolysis and gasification. Energy 2017;125:327–36. https://doi.org/10.1016/j.energy.2017.02.132.

[12] Gassner M, Maréchal F. Thermo-economic optimisation of the integration of electrolysis in synthetic natural gas production from wood. Energy 2008;33:189–98. https://doi.org/10.1016/j.energy.2007.09.010.

[13] Clausen LR, Butera G, Jensen SH. High efficiency SNG production from biomass and electricity by integrating gasification with pressurized solid oxide electrolysis cells. Energy 2019. https://doi.org/10.1016/j.energy.2019.02.039.

[14] Clausen LR, Butera G, Jensen SH. Integration of anaerobic digestion with thermal gasification and pressurized solid oxide electrolysis cells for high efficiency bio-SNG production. Energy 2019;188:116018. https://doi.org/10.1016/j.energy.2019.116018.

[15] Kofler R, Butera G, Jensen SH, Clausen LR. Novel hybrid electricity storage system producing synthetic natural gas by integrating biomass gasification with pressurized solid oxide cells. In: ECOS 2019 - proc. 32nd int. Conf. Effic. Cost, optim. Simul. Environ. Impact energy syst; 2019.

[16] Semelsberger TA, Borup RL, Greene HL. Dimethyl ether (DME) as an alternative fuel. J Power Sources 2006;156:497–511. https://doi.org/10.1016/j.jpowsour.2005.05.082.

[17] Clausen LR, Elmegaard B, Houbak N. Technoeconomic analysis of a low CO2 emission dimethyl ether (DME) plant based on gasification of torrefied biomass. Energy 2010;35:4831–42. https://doi.org/10.1016/j.energy.2010.09.004.

[18] Clausen LR, Elmegaard B, Ahrenfeldt J, Henriksen U. Thermodynamic analysis of small-scale dimethyl ether (DME) and methanol plants based on the efficient two-stage gasifier. Energy 2011;36:5805–14. https://doi.org/10.1016/j.energy.2011.08.047.

[19] Pozzo M, Lanzini A, Santarelli M. Enhanced biomass-to-liquid (BTL) conversion process through high temperature co-electrolysis in a solid oxide electrolysis cell (SOEC). Fuel 2015;145:39–49. https://doi.org/10.1016/j.fuel.2014.12.066.

[20] Aspen Technology. Aspen Plus. https://www.aspentech.com/en/products/engineering/aspen-plus; 2020.

[21] Kaushal P, Proell T, Hofbauer H. Application of a detailed mathematical model to the gasifier unit of the dual fluidized bed gasification plant. Biomass Bioenergy 2011;35:2491–8. https://doi.org/10.1016/j.biombioe.2011.01.025.

[22] Butera G, Gadsbøll RØ, Ravenni G, Ahrenfeldt J, Henriksen UB, Clausen LR. Thermodynamic analysis of methanol synthesis combining straw gasification and electrolysis via the low temperature circulating fluid bed gasifier and a char bed gas cleaning unit. Energy 2020:199. https://doi.org/10.1016/j.energy.2020.117405.

[23] Butera G, Højgaard Jensen S, Østergaard Gadsbøll R, Ahrenfeldt J, Røngaard Clausen L. Flexible biomass conversion to methanol integrating solid oxide cells and TwoStage gasifier. Fuel 2020:271. https://doi.org/10.1016/j.fuel.2020.117654.

[24] Gadsbøll RØ, Clausen LR, Thomsen TP, Ahrenfeldt J, Henriksen UB. Flexible TwoStage biomass gasifier designs for polygeneration operation. Energy 2019;166:939–50. https://doi.org/10.1016/j.energy.2018.10.144.

[25] Trinh TN, Jensen PA, Dam-Johansen K, Knudsen NO, Sørensen HR, Hvilsted S. Comparison of lignin, macroalgae, wood, and straw fast pyrolysis. Energy Fuels 2013;27:1399–409. https://doi.org/10.1021/ef301927y.

[26] Channiwala SA, Parikh PP. A unified correlation for estimating HHV of solid , liquid and gaseous fuels q. Fuel 2002;81:1051–63.

[27] Clausen LR. Maximizing biofuel production in a thermochemical biorefinery by adding electrolytic hydrogen and by integrating torrefaction with entrained flow gasification. Energy 2015;85:94–104. https://doi.org/10.1016/j.energy.2015.03.089.

[28] Vad Mathiesen B, Ridjan I, Connolly D, Nielsen MP, Hendriksen Vang P, Bjerg Mogensen M, et al. Technology data for high temperature solid oxide electrolyser cells , alkali and PEM electrolysers. 2013.

[29] Ahrenfeldt J, Henriksen U, Jensen TK, Gøbel B, Wiese L, Kather A, et al. Validation of a continuous combined heat and power (CHP) operation of a two-stage biomass gasifier. Energy Fuels 2006;20:2672–80. https://doi.org/10.1021/ef0503616.

[30] Duret A, Friedli C, Maréchal F. Process design of Synthetic Natural Gas (SNG) production using wood gasification. J Clean Prod 2005;13:1434–46. https://doi.org/10.1016/j.jclepro.2005.04.009.

[31] Bühler F. Energy efficiency in the industry: a study of the methods, potentials and interactions with the energy system. Technical University of Denmark; 2018.

[32] Dupont C, Chiriac R, Gauthier G, Toche F. Heat capacity measurements of various biomass types and pyrolysis residues. Fuel 2014;115:644–51. https://doi.org/10.1016/j.fuel.2013.07.086.

[33] Lehto J, Oasmaa A, Solantausta Y, Kytö M, Chiaramonti D. Review of fuel oil quality and combustion of fast pyrolysis bio-oils from lignocellulosic biomass. Appl Energy 2014;116:178–90. https://doi.org/10.1016/j.apenergy.2013.11.040.

[34] Butera G, Fendt S, Jensen SH, Ahrenfeldt J, Clausen LR. Flexible methanol production units coupling solid oxide cells and thermochemical biomass conversion via different gasification technologies. Energy 2020;208:118432. https://doi.org/10.1016/j.energy.2020.118432.